



## Effect of microscale compressibility on apparent porosity and permeability in shale gas reservoirs



Guanglong Sheng<sup>a,b</sup>, Farzam Javadpour<sup>b,\*</sup>, Yuliang Su<sup>a,\*</sup>

<sup>a</sup> School of Petroleum Engineering, China University of Petroleum (East China), No. 66, Changjiang West Road, Huangdao District, Qingdao 266580, China

<sup>b</sup> Bureau of Economic Geology, Jackson School of Geosciences, The University of Texas at Austin, Austin, TX 78713, USA

### ARTICLE INFO

#### Article history:

Received 15 August 2017

Received in revised form 18 November 2017

Accepted 2 December 2017

#### Keywords:

Shale reservoirs  
Stress sensitivity  
Compressibility  
Apparent porosity  
Apparent permeability

### ABSTRACT

The pore network in shale reservoirs comprise of nanoporous organic matter (OM) and micron-size pores in inorganic material (iOM). Accurate gas transport models in shale must include gas slippage, Knudsen diffusion, surface diffusion, and sorption. The change in pore size due to the applied stress could consequently affect gas transport processes. In this study we a compression coefficient to characterize the influence of stress sensitivity on key parameters for gas transport. We consider separate stress response in nanoporous organic matter and iOM because of their different mechanical properties. The effects of compressibility on apparent permeability of OM and iOM are analyzed at different pore sizes, pore pressures and for different gas compositions. Our results show that compressibility has a greater influence on the apparent permeability of iOM than on OM when pore sizes are smaller than 10 nm, whereas compression has similar impact on apparent permeability of both media when pore sizes are larger than 10 nm. With the same effective stress, lower pore pressure results in greater impair in permeability. We conducted a reservoir simulation study using conventional dual-continua model with our developed pressure dependent porosity and permeability to showcase field implication of this study. This work is an important and timely investigation of the development of shale-reservoir-flow simulators.

© 2017 Elsevier Ltd. All rights reserved.

### 1. Introduction

Shale gas reservoirs are composed mainly of OM and iOM. Research shows that pore sizes in shale gas reservoirs range from 1 to 200 nm [26,28,56,58,59] and that organic pores are usually smaller than 10 nm in diameter [3,41,45,46]. The mechanisms of gas migration in microscale pores, which differ from those in conventional reservoirs (Fig. 1), include viscous flow with slippage, Knudsen diffusion, surface diffusion, and gas adsorption and desorption [1,13,16,20,29,33,49,57,64]. Unlike conventional reservoirs, migration of shale gas in microscale media is strongly influenced by factors such as absorbed gas, pore pressure, pore size, and properties of porous media. Therefore, the conventional Darcy equation and intrinsic-property parameters of a reservoir (such as permeability and porosity) are no longer applicable for describing complex gas- transport mechanisms in shale reservoirs.

In recent years, researchers have introduced “apparent permeability” for shale gas reservoirs to describe gas transport in microscale pores. Javadpour [20] first introduced an apparent-

permeability model that couples viscous flow and Knudsen diffusion in nanopores by comparing formulation for gas flow with the Darcy equation. On the basis of the Javadpour model, many scholars have developed numerous shale models that can couple complex gas-transport mechanisms by apparent permeability. Present-day apparent-permeability models for shale gas reservoirs can be divided into the following three types:

- Javadpour models based on the pore radius of porous media [1,2,20,33–34,36,47,62]
- Civan models based on Knudsen number [11,12,19,38,40,44,49,54]
- The Dusty-Gas Model (DGM) based on diffusion coefficient [17,22,25,27,52,61]

Javadpour models characterize intrinsic permeability, Knudsen diffusion coefficient, and slip factor using pore size and propose coupled-flow equations considering viscous flow, slippage effect, Knudsen diffusion, and surface diffusion. Civan models apply the Beskok model [5] to describe gas migration in porous media and use the Knudsen number in models to couple viscous flow and Knudsen diffusion. The DGM couples viscous flow, Knudsen diffusion, and molecular diffusion in porous media. In the DGM,

\* Corresponding authors.

E-mail addresses: [farzam.javadpour@beg.utexas.edu](mailto:farzam.javadpour@beg.utexas.edu) (F. Javadpour), [suyuliang@upc.edu.cn](mailto:suyuliang@upc.edu.cn) (Y. Su).

**Nomenclature**

|             |  |                    |  |
|-------------|--|--------------------|--|
| $C_g$       | gas compressibility, $\text{MPa}^{-1}$   | $p_m$              | pressure in iOM, MPa   |
| $C_k$       | OM total compressibility, $\text{MPa}^{-1}$  | $p_L$              | Langmuir's pressure, MPa   |
| $C_m$       | iOM total compressibility, $\text{MPa}^{-1}$                                       | $r_k$              | effective radius of pores in OM, m                                       |
| $c_{\mu s}$ | Langmuir volume on the OM surface, $\text{mol}/\text{m}^3$                         | $r_{k\_ini}$       | initial effective radius of pores in OM, m                               |
| $c_k$       | amount of free gas in unit OM, $\text{mol}/\text{m}^3$                             | $r_{m\_ini}$       | initial radius of pores in iOM, m  |
| $c_{\mu}$   | amount of adsorbed gas in unit OM, $\text{mol}/\text{m}^3$                         | $R$                | universal gas constant, $8.314 \text{ J}/(\text{K}\cdot\text{mol})$      |
| $c_m$       | amount of free gas in unit iOM, $\text{mol}/\text{m}^3$                            | $T$                | formation temperature, K   |
| $D_{k\_kn}$ | Knudsen diffusion coefficient of OM, $\text{m}^2/\text{s}$                         | $Z$                | compression factor   |
| $D_{km}$    | Knudsen diffusion coefficient of iOM, $\text{m}^2/\text{s}$                        | $\phi_k$           | effective intrinsic porosity of OM                                       |
| $D_s$       | surface diffusion coefficient of OM, $\text{m}^2/\text{s}$                         | $\phi_{k\_ini}$    | effective initial intrinsic porosity of porous kerogen                   |
| $D_{s,0}$   | surface diffusion coefficient of OM at zero loading, $\text{m}^2/\text{s}$         | $\phi_m$           | intrinsic porosity of iOM  |
| $f$         | tangential momentum accommodation coefficient (TMAC)                               | $\tau_k$           | tortuosity correction factor of OM                                       |
| $k_{kv}$    | intrinsic permeability of OM, $\text{m}^2$   | $\tau_m$           | tortuosity correction factor of iOM                                      |
| $M$         | molecular weight, $\text{kg}/\text{mol}$   | $\mu_g$            | gas viscosity, $\text{mPa}\cdot\text{s}$                                 |
| $N_{k\_kn}$ | flux for Knudsen diffusion of free gas, $\text{mol}/(\text{m}^2\cdot\text{s})$     | $\varepsilon_{ks}$ | proportion of solid OM volume in total interconnected matrix pore volume |
| $N_{k\_vs}$ | flux for slippage viscous flow of free gas, $\text{mol}/(\text{m}^2\cdot\text{s})$ | $\theta_k$         | the surface coverage of the adsorption layer on the porewall             |
| $N_{k\_su}$ | flux for surface diffusion of adsorbed gas, $\text{mol}/(\text{m}^2\cdot\text{s})$ |                    |  |
| $p_{ini}$   | initial pressure in reservoir, MPa   |                    |  |
| $p_k$       | pressure in OM, MPa  |                    |  |

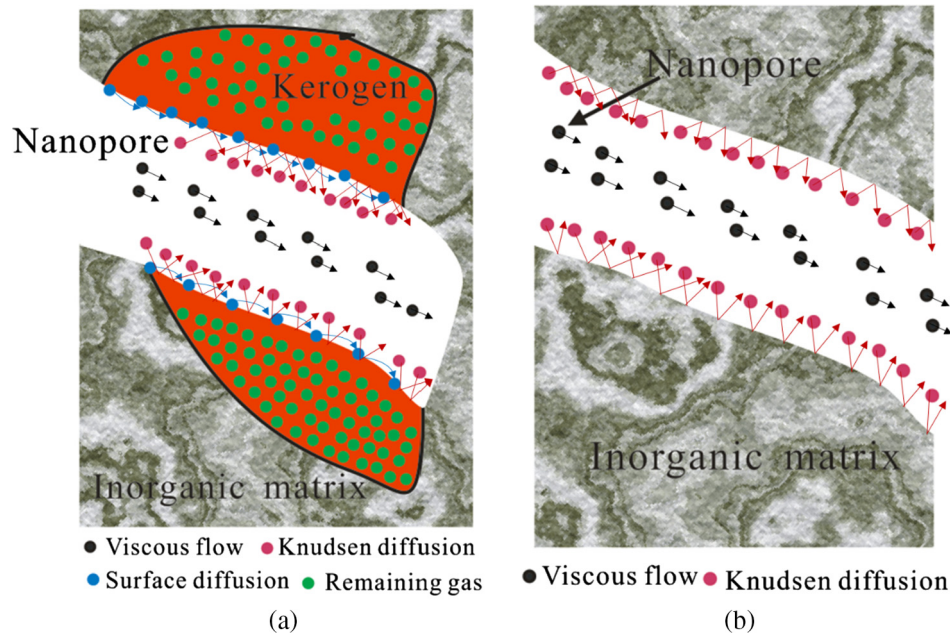


Fig. 1. Mechanisms of shale gas migration in (a) OM, and (b) iOM.

apparent permeability is presented in the form of the Klinkenberg effect for one-component gas in shale gas reservoirs with viscous flow and Knudsen diffusion.

Extensive research has shown that apparent permeability of shale gas reservoirs is affected by many factors, including pore pressure, reservoir temperature, surface roughness, and phase change [8,14,37,43,60].

Stress sensitivity is the effect of pore-throat shrinkage on permeability. During depressurization development, effective stress increases, resulting in the rearrangement and crushing of matrix particles. Stress sensitivity of rock occurs with specific petrophysical phenomena, including decreases in pore size, intrinsic porosity, and intrinsic permeability [50]. Compared with sandstone, shale matrix strength is weaker with more deformation, and the

effect on stress sensitivity is stronger [15,48]. Related experiments showed that permeability and porosity decrease significantly with the increase of effective stress in shale reservoirs [2,10,15,30]. When Dong et al. [15] measured stress-dependent permeability and porosity, results showed that permeability of shale was more sensitive to effective confining pressure than was permeability of sandstone, while sandstone and shale showed a similar sensitivity of porosity to effective pressure. Dong et al. [15] results also indicated that power law can be used to characterize regularity permeability and porosity with stress dependence.

Mokhtari et al. [30] characterized natural or induced fractures in several shale reservoirs using computed tomography (CT) scans in various resolutions and evaluated the effect of stress on permeability. Results showed that effective permeability to gas declined

Download English Version:

<https://daneshyari.com/en/article/7054520>

Download Persian Version:

<https://daneshyari.com/article/7054520>

[Daneshyari.com](https://daneshyari.com)